

# QUANTITATIVE ANALYSIS OF GAS CIRCUIT BREAKER PHYSICS THROUGH DIRECT COMPARISON OF 3D SIMULATIONS TO EXPERIMENT

N.P. Basse<sup>‡</sup>, M. Abrahamsson, M. Seeger, T. Votteler  
ABB Switzerland Ltd., Corporate Research, Segelhofstrasse 1  
CH-5405 Baden-Dättwil, Switzerland

## Abstract

Understanding the dynamic processes governing gas circuit breaker physics is crucial in order to continue to improve short-circuit current interruption performance.

In this contribution we study a single arc discharge both using measurements and three-dimensional computational fluid dynamics simulations. The primary quantity analyzed is the pressure in the heating volume created by radiative ablation of the Polytetrafluoroethylene nozzles surrounding the arc. We use cross correlation functions to investigate the behavior of pressure waves in the SF<sub>6</sub> gas, especially those induced at flow reversal where the gas flow between the arc zone and heating volume changes direction.

## I. INTRODUCTION

The arc zone of high voltage self-blast gas circuit breakers is challenging to diagnose directly due to the combination of temperatures in the 30,000 K range and densities of order 10<sup>25</sup> m<sup>-3</sup>. Instead, proxy measurements are made, typically in the heating volume of the breakers. In this contribution we compare pressure measurements of the SF<sub>6</sub> gas from two sensors to three-dimensional (3D) computational fluid dynamics (CFD) simulations. The simulated pressure evolution is analyzed at the same position as the actual sensors are placed, so in that sense the CFD simulations can be thought of as a synthetic diagnostic. The overarching purpose of this quantitative comparison of CFD simulations with measurements is to improve our understanding of the physics of current interruption in gas circuit breakers. Further, questions will be generated in the case where agreement is poor between simulation and experiment. This in turn guides us as to what should be (i) modified in the simulation and/or (ii) additionally measured to answer the questions posed and thereby improve our knowledge of the physical processes.

The paper is organized as follows: In Sec. II we describe the arc discharge treated; we introduce the 3D CFD simulation in Sec. III. The comparison between measured and simulated heating volume pressures is to be found in Sec. IV.

## II. DISCHARGE DESCRIPTION

The basic layout of a gas circuit breaker is shown in Fig. 1; only the upper half of the breaker is shown. Initially, the plug contact is physically touching the finger contact (or tulip). When high current is to be interrupted, the contacts separate and an arc forms between them. The sequence of events leading to current interruption is the following:

1. Radiation from the arc causes ablation of the Polytetrafluoroethylene (PTFE) nozzle, leading to flow from the high pressure arc zone to the heating volume; this is known as backheating. In the case of high current, the arc is said to be ablation controlled at this time [2].
2. Pressure increases in the heating volume and begins to decrease in the arc zone as current zero (CZ) is approached and ablation is reduced. At the time when the heating volume pressure equals the arc zone pressure flow reversal takes place.
3. Flow is thereafter directed from the heating volume to the arc zone and the arc is axially blown [3].
4. The arc is extinguished at CZ.

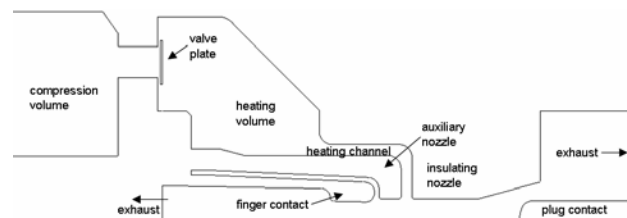
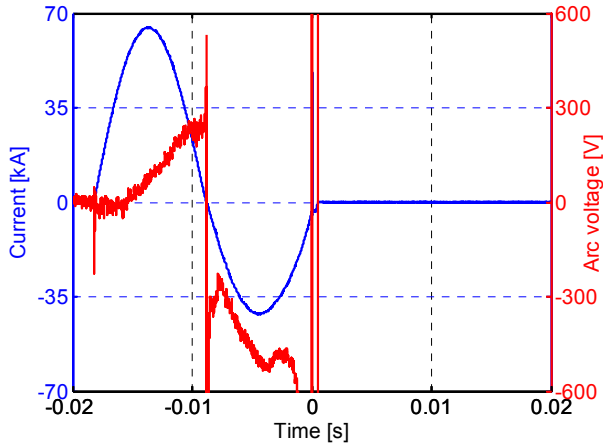


Figure 1. Gas circuit breaker sketch [1].

Arc current and voltage for the discharge analyzed is shown in Fig. 2. Current is limited to two half-waves by a vacuum circuit breaker. CZ is after the second half-wave at zero seconds on the time axis. The rise of the arc voltage defines the time of contact separation, leading to an arcing time of 15 ms. The current peaks are strongly asymmetric due to the setup of the test circuit.

<sup>‡</sup> email: nils.basse@ch.abb.com



**Figure 2.** Arc current (blue) and voltage (red).

The measured heating volume pressure using sensors hv1 and hv2 is shown in Fig. 3. The qualitative behavior is the same for the two measurements, with a maximum pressure of about 25 bar a few ms after the peak of the second current half-wave. Pronounced oscillations are observed both during the high current phase and after CZ.

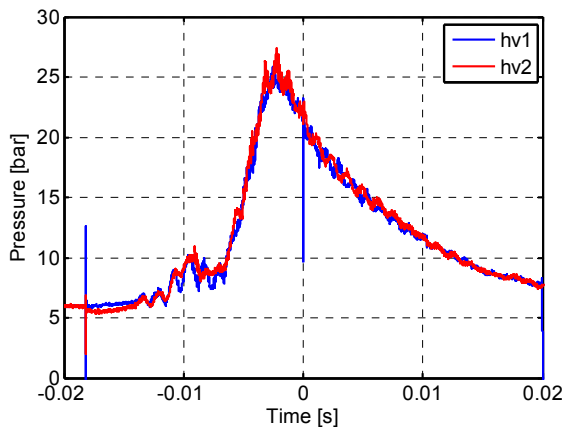


**Figure 3.** Measured heating volume pressure using sensors hv1 (blue) and hv2 (red).

### III. CFD SIMULATION

Part of the CFD simulation domain is shown in Fig. 4; the total number of cells simulated is about 250,000. The physical model used in the simulation is a two-zone model [4], where the arc zone is divided into two isothermal zones: (i) A conducting arc zone and (ii) a non-conducting PTFE vapor layer surrounding the arc. Turbulence is not included in the simulation. At the time displayed a pressure wave in the heating volume can clearly be seen originating where the heating channel is connected to the heating volume. We use simulated

pressure at monitor points 1 and 21 and compare to the two measurements, also positioned 180 degrees apart.

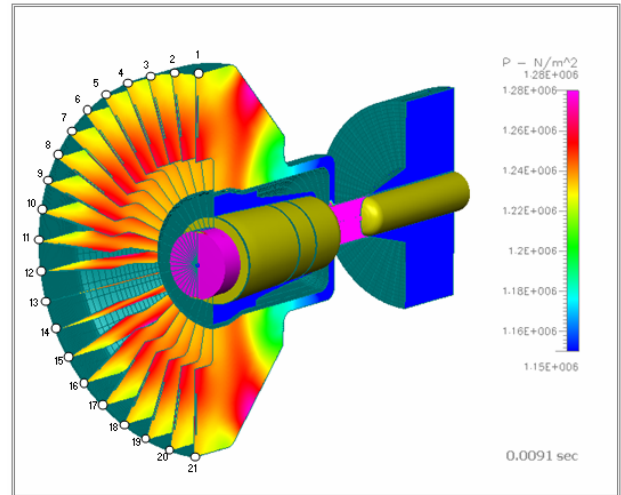


**Figure 4.** Simulated pressure with the 21 pressure monitor points marked.

The simulated pressure in the arc zone at the stagnation point (sp) and at one of the monitor points in the heating volume (p1) is shown in Fig. 5. The stagnation point is situated where the heating channel joins the arc zone. Therefore the pressure at this position is zero until the plug has moved past the stagnation point. After this occurs, the stagnation point pressure jumps up to the arc zone pressure. Flow reversal takes place 2 ms before CZ.

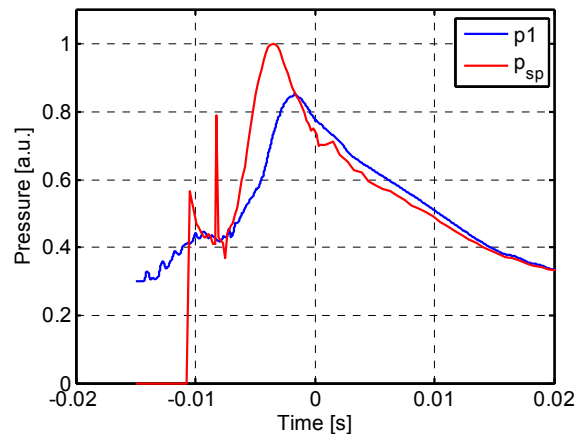


**Figure 5.** Heating volume pressure at monitor point 1 ( $p_1$ , blue) and at the stagnation point of the arc zone ( $p_{sp}$ , red).

To quantify the transient behavior associated with flow reversal, we calculate the cross correlation function between the heating volume and arc zone pressures, see Fig. 6. A negative timelag means that the event first takes place in the heating volume, thereafter in the arc zone.

Two features can be observed:

1. At -6 ms a correlated (red), oscillating structure is seen. The peak is at zero timelag, so the event is occurring at the same time for both positions. The period can be estimated to 2.8 ms from the anti-correlated (blue), symmetric troughs at +/- 1.4 ms.
2. At -2 ms an anti-correlated, oscillating structure is seen, The peak is at -0.2 ms and the period is roughly as before, namely 2.8 ms.

The transition between these two features coincides with the flow reversal time and the second feature can be interpreted as a simultaneous reduction of the heating volume pressure and small increase of the arc zone pressure (anti-correlation).

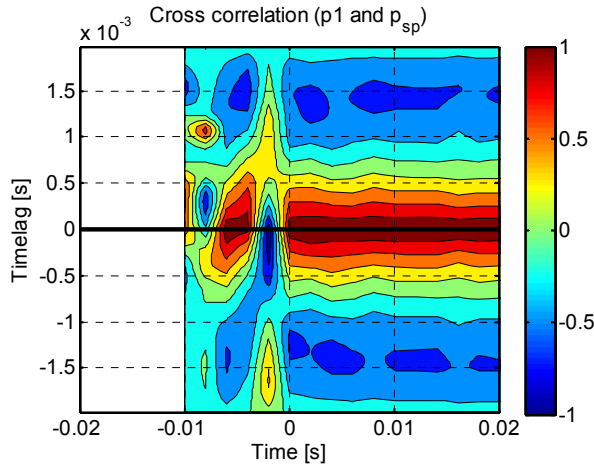


**Figure 6.** Cross correlation function between simulated heating volume and arc zone pressure. Red (blue) is due to correlated (anti-correlated) structures.

The physical processes from flow reversal onwards can be understood as follows:

1. Hot (about 5000 K) gas from the heating channel begins to flow to the arc zone because of the pressure reduction there.
2. Outflow of colder ( $< 2000$  K) gas from the heating volume starts, highly subsonic at first.
3. The pressure increases slightly in the arc zone, but remains below the heating volume pressure because of energy dissipation in the heating channel.
4. Flow from the heating volume to the arc zone stops and the arc zone pressure decreases.
5. When the arc zone pressure is below the heating channel pressure by a certain amount, cold gas from the heating channel flows to the arc zone and stops the pressure decay there.
6. A smaller increase of the arc zone pressure occurs and the cycle starts again.
7. Since these cycles are in cold gas at this late time, oscillation amplitudes are low and heavily damped.

#### IV. COMPARISON BETWEEN MEASUREMENT AND SIMULATION

The cross correlation between the simulated pressure at monitor points 1 and 21 is shown in Fig. 7.

Three pressure oscillations can be identified:

1. A feature at -12 ms with a period of 2.4 ms.
2. A feature at -5 ms with a period of 2.6 ms.
3. A feature after CZ with a period of 2.8 ms.

The first two features are associated with the two current half-waves and the resulting pressure buildup. The final oscillations after CZ are in cold gas.

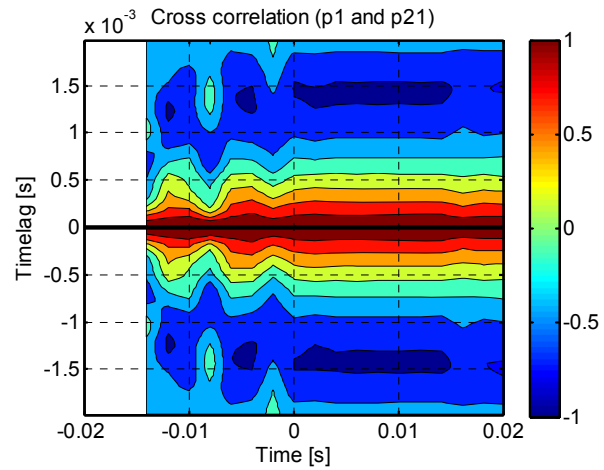


**Figure 7.** Cross correlation function between simulated heating volume pressure in monitor points 1 and 21.

The cross correlation in Fig. 7 can be directly compared to the cross correlation between the measured heating volume pressures 180 degrees apart, see Fig. 8.

Features 2 and 3 from Fig. 7 are also observed in the measurements with the same period.

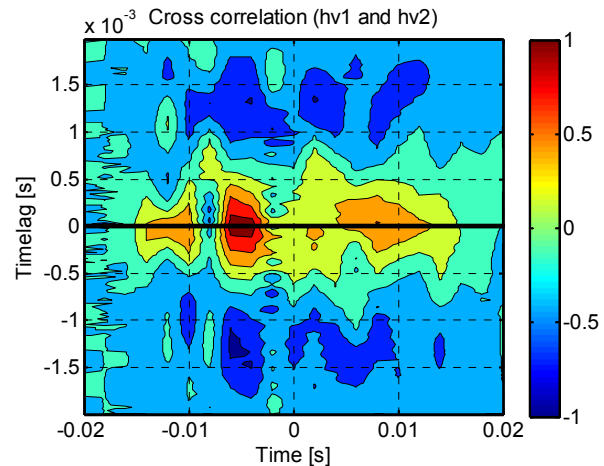


**Figure 8.** Cross correlation function between measured heating volume pressure 180 degrees apart.

One can combine information on the oscillation periods found above with the circuit breaker geometry and simulated pressure using four steps:

1. The distance between the heating volume pressure sensor location and the stagnation point along with the time delay between them is used to construct the average velocity,  $v_{average}$ , between the two points.
2. The simulated ratio between the arc zone and heating volume pressures can be used to construct the Mach number ( $Ma$ ) between the locations according to

$$\left( \frac{p_{position1}}{p_{position2}} \right)^{\frac{\gamma-1}{\gamma}} = 1 + \frac{\gamma-1}{2} \times Ma^2, \quad (1)$$

where  $\gamma$  is the adiabatic coefficient, see Fig. 9 [5]. We take  $\gamma$  to be 1.1, which is the value for 1500 K. The Mach number is quite insensitive to the chosen  $\gamma$ .

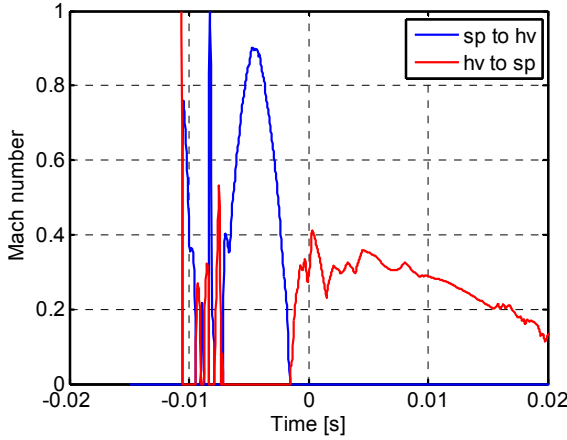


**Figure 9.** Mach number found from the CFD simulation and Eq. (1). The blue line is flow from the arc zone to the heating volume and the red line is flow from the heating volume to the arc zone.

3. The sound speed is found from

$$v_{sound} = \frac{v_{average}}{Ma}. \quad (2)$$

4. The calculated sound speed yields the average temperature. In Fig. 10 we show the sound speed vs. temperature for pressures of 1 and 25 bar. The sound speed is independent of pressure up to 1500

K and increases with the square root of temperature.

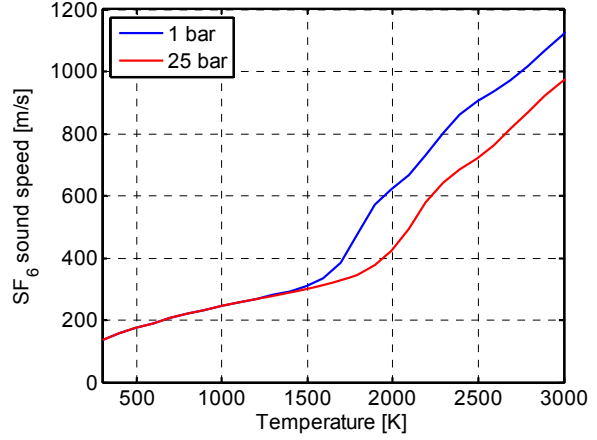


**Figure 10.** Sound speed vs. temperature for 1 bar (blue) and 25 bar (red).

Using this technique we calculate the average temperature for feature 3, see Figs. 7 and 8. The average speed is of the order 100 m/s and we derive the following temperature:  $T_{feature\ 3} = 1600$  K. The average simulated heating volume temperature for the feature is about 1200 K, see Fig. 11.

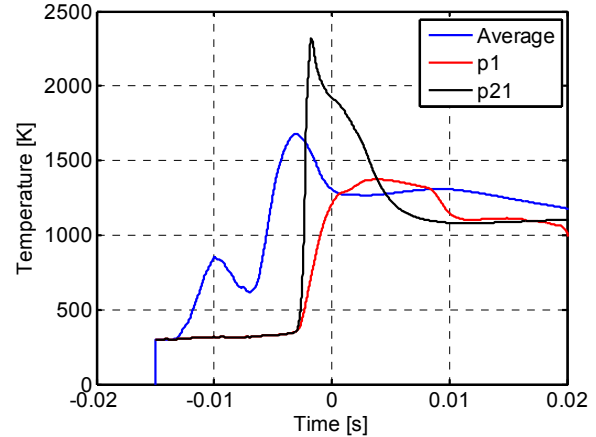


**Figure 11.** Simulated temperatures: Average in heating volume (blue) and at pressure sensor location 1 (red) and 21 (black).

Our simple estimate of an average temperature from a combination of simulation and measurements is a basic consistency check and shows that discrepancies exist. Temperature measurements are needed to address this issue quantitatively. Modifications to the simulation include (i) a more exact treatment of the arc radiation and (ii) addition of a realistic turbulence model.

## V. REFERENCES

- [1] C. M. Franck and M. Seeger, "Application of high current and current zero simulations of high-voltage circuit breakers," *Contrib. Plasma Phys.*, vol. 46, pp. 787-797, 2006.
- [2] M. Seeger, L. Niemeyer, T. Christen, M. Schwinne, and R. Dommerque, "An integral arc model for ablation controlled arcs based on CFD simulations," *J. Phys. D: Appl. Phys.*, vol. 39, pp. 2180-2191, 2006.
- [3] W. Hermann, U. Kogelschatz, K. Ragaller, and E. Schade, "Investigation of a cylindrical, axially blown, high-pressure arc," *J. Phys. D: Appl. Phys.*, vol. 7, pp. 607-619, 1974.
- [4] L. Niemeyer, "Evaporation dominated high current arcs in narrow channels," *IEEE Trans. Power App. Syst.*, vol. PAS-97, pp. 950-958, 1978.
- [5] R. D. Blevins, *Applied Fluid Dynamics Handbook*. Van Nostrand Reinhold, New York, New York, USA, 1984.